


Original research article

A novel IgG Fc by computer-aided design enhances heavy-chain heterodimerization in bi- or trispecific antibodies

Bo Wang^{1,†}, Jun Lin^{2,4,†}, Matthew R. Hoag¹, Meredith Wright¹, Mingjun Ma², Wenyan Cai¹, Sachith Gallolu Kankanamalage¹  and Yue Liu^{1,3,*}

¹Ab Studio, Inc., Hayward, CA 94545, USA, ²Genor Biopharma Co. Ltd., Shanghai 201203, P.R.C., ³Ab Therapeutics, Inc., Hayward, CA 94545, USA, and ⁴Department of Biological Medicines & Shanghai Engineering Research Center of Immunotherapeutics, Fudan University School of Pharmacy, Shanghai 201203, P.R.C.

Received: March 4, 2022; Revised: June 24, 2022; Accepted: July 21, 2022

ABSTRACT

The classical ‘knob-into-holes’ (KIH) strategy (knob(T366Y)/hole (Y407T)) has successfully enhanced the heterodimerization of a bispecific antibody (BsAb) resulting in heterodimer formation up to 92% of protein A (ProA)-purified protein pool. However, it does not show high efficiency for every BsAb. KIH was initially applied to a CD20/CD3 BsAb. After *in silico* modeling, two additional new mutations, S354Y in knob-heavy chain (HC) and Q347E in hole-HC, together with KIH named ‘ETYY’, were introduced in the Fc. The CD20/CD3 BsAb hybrid only represented ~50% of the ProA-purified protein pool when KIH was applied. With ETYY, the percentage of CD20/CD3 hybrid increased to 93.8%. CD20/CD3-v4b (containing ETYY) retains the original activity of the BsAb at both Fab and Fc regions, and also shows good developability. These results indicate that the computer-aided novel ETYY design has the potential to improve the development of next-generation BsAbs with higher yields and simpler purification.

Statement of Significance: The computationally designed novel ETYY mutations improve heterodimer formation in multi-specific antibodies while preserving the functional and physicochemical properties. This could greatly enhance the large-scale manufacturability and ease of purification for multi-specific antibodies for which heterodimerization is necessary.

KEYWORDS: Fc engineering; knob-into-hole; bispecific antibodies; trispecific antibodies; computer-aided antibody design; heavy chain heterodimerization; multi-specific antibodies

INTRODUCTION

Bispecific antibodies (BsAbs) were first introduced by Nisonoff [1] and show vast potential in the treatment of human diseases, especially for different types of cancer. However, during the production of recombinant BsAbs (the type discussed in this paper is an IgG-like BsAb with two heavy chains [HCs] and one common light chain [LC]) using ectopic gene expression, a significant proportion of homodimers of the two antibody HCs can also be

generated in addition to the expected heterodimers, leading to low-efficiency BsAb production and more difficult purification/separation.

‘Knobs-into-holes’ (KIH) was originally proposed by Crick [2] as a model for the packing of amino acid side chains between adjacent α -helices. Ridgway *et al.* [3] from Genentech introduced this strategy to IgG Fc engineering for the heterodimerization of BsAbs. In this strategy, a pair of mutations, knob (T366Y) and hole (Y407T), were applied to the Fc domain of the BsAb. It greatly facili-

*To whom correspondence should be addressed. Yue Liu, Ab Studio, Inc., Hayward, CA 94545, USA. Email: yue.liu@antibodystudio.com

†These authors contributed equally to the work included in the manuscript.

© The Author(s) 2022. Published by Oxford University Press on behalf of Antibody Therapeutics. All rights reserved. For Permissions, please email: journals.permissions@oup.com

This is an Open Access article distributed under the terms of the Creative Commons Attribution Non-Commercial License (<http://creativecommons.org/licenses/by-nc/4.0/>), which permits non-commercial re-use, distribution, and reproduction in any medium, provided the original work is properly cited. For commercial re-use, please contact journals.permissions@oup.com

tated the heterodimerization of the BsAb, increasing the heterodimer level of this BsAb from 57% to 92% in the protein A (ProA)-purified protein pool [3].

Since then, this strategy has been used extensively to design bispecific, multispecific and even monovalent antibodies, and there is a breadth of examples in literature [2–20]. Antibodies produced using this strategy are currently in clinical use [4–8], and many others are in clinical development [9]. The traditional KIH strategy was integral in the development of more complex bispecific antibody (BsAb) platforms such as CrossMab and DuetMab [9–11] and has been used in conjunction with ‘electrostatic steering’ approaches for even greater effectiveness [12]. In addition, this strategy has proven its flexibility in that it has been used effectively to produce BsAbs in a variety of protein expression systems including mammalian-cell-based systems, bacterial-cell-based systems [13] and even in cell-free systems [14]. Time-tested and proven to be effective; this strategy has the potential to become a core component in multispecific antibody design and development.

However, while the example BsAb hybrid in the original 1996 study made up 92% of the ProA-purified protein pool, this knob (T366Y)/hole (Y407T) design may result in lower efficiencies for other BsAbs. For instance, when this strategy was applied to an in-house CD20/CD3 BsAb, the BsAb hybrid represented only ~50% of the ProA purified protein pool, and therefore, additional design was pursued to increase the purity of the BsAb hybrid and simplify purification and downstream processing. In our 2021 paper by Cai *et al.* [15], we describe the excellent pharmacological properties of this CD20/CD3 BsAb, while leaving out details of the ETTY design itself. We describe the ETTY design in detail here, outline its development and review its applicability. Here, we used 3D modeling and computational design to identify and introduce another two mutations within the CH3 domains of the BsAb Fc, in addition to the original KIH mutations (ETYY mutations) [15]. Then, the formation of heterodimer and homodimers was assessed by ProA purification, ion exchange chromatography purification and some related assays. The results indicate that the engineered Fc with the classical KIH and two additional mutations significantly increases the heterodimerization in the final product, and this serves as a case study in the computer-aided engineering of antibodies within the Fc region to improve manufacturability.

MATERIALS AND METHODS

Computer-aided IgG Fc design

The Fc/Fc interface of a human IgG1(pdb 1HZH) 3D structure was modeled by Schrodinger BioLuminate. Interface residues were highlighted and served as objectives for *in silico* mutations. CH2 was not considered for mutation since many Fc functions, such as ADCC and CDC, are dependent on the structure of the CH2 domain. The criteria for mutational design of the interface residues are: (1) if the distance between the residues forming an interchain

interaction is too long (>4 Angstroms), they will not be selected for mutation, in order to avoid structural change; (2) if the distance between the residues forming an inter-chain interaction is moderate (<4 Angstroms), *in silico* mutations will be designed and analyzed (both biophysically and biochemically) to result in a new or stronger interaction (including ionic bonding, hydrophobic interaction or hydrogen bonding) without major changes to Fc/Fc structure.

Construction of HC variants on CH3

A CD20/CD3 BsAb, which included an CD20 HC, an CD3 HC and a common LC, was used in this study. Mutations were introduced in the CH3 domain of the BsAb, including the classic KIH of ‘knob (T366Y)/hole (Y407T)’, and the two additional new mutations of S354Y in knob-HC and Q347E in hole-HC. Site-directed mutagenesis was applied to the parental plasmid for the generation of the Fc mutations by polymerase chain reaction. The mutant plasmids were verified by sequencing (Elim Biopharm, Hayward, CA).

Expression and purification of CD20/CD3 IgG-like BsAb

The plasmids encoding the CD20 HC, CD3 HC and their common LC were co-transfected into Expi293F cells using the ExpiFectamine 293 Transfection Kit (Thermo Fisher), and enhancers were added after 17 h according to manufacturer’s instructions. The plasmids were used in transfection at 1 μ g per 3×10^7 [7] cells (in 1 mL), and the ratio of CD20-HC: CD3 HC: Common LC was 1:1:5. Seventy-two hours after transfection, the cells were centrifuged at 3000 g for 10 min. The supernatant was obtained and filtered with a 0.45- μ m membrane, and the CD20/CD3 BsAb concentration was measured using ProA probe on the Gator instrument (Gator Bio). Then, the BsAb was purified using ProA column on the AKTA Explorer 100 purification system (buffer A: phosphate-buffered saline [PBS], pH = 7.4; buffer B: 0.1 M Glycine, pH = 2.5) and dialyzed in PBS (8.1 mM Na₂HPO₄, 1.9 mM KH₂PO₄, 137 mM NaCl, 2.7 mM KCl, pH = 7.4) or tris buffer (TB) (20 mM Tris-Cl, pH = 9) twice. Anion exchange chromatography (AEX, Mono S 5/50 GL, Sigma-Aldrich) was applied to further separate the heterodimer from homodimer with a salt gradient (Buffer A: 20 mM Tris-Cl buffer, pH = 9; Buffer B: 20 mM Tris-Cl, 1 M NaCl, pH = 9; gradient: 0–25% buffer B in 40 min). The purified BsAb was dialyzed in PBS twice and filtered with a 0.22- μ m membrane.

Mass spectrometry (MS) analysis

For intact or deglycosylated mass analysis, the protein was first diluted to 0.5 mg/mL with 50 mM Tris-HCl. In the case of deglycosylated mass analysis. A total of 1 μ L of PNGase F was then added to 100 μ L of the diluted protein solution and the mixture was incubated at 37°C for 2 h. To quench the reaction, trifluoroacetic acid (FA) was added to a final concentration of 0.25%. For denatured

and reduced mass analysis, 1 μL (20 μg) of the protein was mixed with 1 μL of 0.5 M Dithiothreitol, 4 μL of Rapid PNGase F buffer (denaturing buffer) and 14 μL of double distilled (DD) water. Then, the mixture was incubated at 75°C for 5 min, cooled and diluted to 0.5 mg/mL with DD water. All the samples were separated on Waters H-Class Bio using a reversed-phase column (Waters BioResolve RP Column). The temperature of the column was maintained at 70°C. Mobile phase A was 0.05% (v/v) TFA in water and mobile phase B was 0.05% (v/v) TFA in acetonitrile. The samples (2.5 μg) were injected and separated using a gradient (held at 20% B for 3 min, 20–32% B for 2 min, then 32–60% B within 13 min). A flow rate of 300 $\mu\text{L}/\text{min}$ was employed. The online liquid chromatography-electrospray ionization-mass spectrometry (LC-ESI-MS) analysis was performed using a Waters SYNAPT G2-Si high-resolution mass spectrometer. The ESI capillary voltage was set at 3.8 KV for intact and deglycosylated mass analysis while 3.5 KV for denatured and reduced mass analysis. The source temperature was set at 120°C and desolvation temperature was set at 250°C. The mass spectrometer was set up to acquire one high-resolution full scan at 10 000 resolution (at m/z 400).

FcRn binding analysis

Neonatal Fc receptor (FcRn) binding analysis was performed on Biacore T200. Human FcRn was immobilized on a CM-5 sensor chip with the target level of about 250 RU. The running buffer was 20 mM sodium phosphate, pH 6.0, 150 mM NaCl, 0.005% polysorbate 20 (PBS-P20). The CD20/CD3 BsAb sample was 2-fold serially diluted from 1000 nM to 62.5 nM. Then, single cycle kinetics was applied with contact time of 50 s for the ascending five concentrations and with a dissociation time of 100 s. The acquired curve was fitted to steady state affinity model and dissociation value (KD) was calculated.

Thermostability assay (DSF/SLS) and aggregation potential assay (DLS)

The purified BsAb samples were submitted to the UNcle system (Unchained Labs) for analysis. Dynamic light scattering (DLS) was measured at 25°C and the data were calculated and analyzed using the UNcle Analysis Software. For differential scanning fluorimetry (DSF)/static light scattering (SLS) assays, a temperature ramp of 1°C/min was performed with monitoring from 25°C to 95°C. SLS was measured by Uncle at 266 and 473 nm. T_m and T_{agg} were also calculated and analyzed by the UNcle Analysis Software.

DSC analysis

Differential scanning calorimetry (DSC) analysis was performed on a MicroCal Capillary VP-DSC. The sample was diluted to 0.5 mg/mL and heated from 25 to 100°C at a heating rate of 60°C/h. Balance time before scanning was 3 min.

RESULTS

Design and 3D modeling of the KIH Fc, CD20/CD3-v2, CD20/CD3-v4b and CD20/CD3-v5b antibodies

The KIH Fc was engineered by 3D modeling and computer-aided design, developed and analyzed. Schrödinger BioLuminate software was used to identify interchain interactions of the wild-type IgG Fc CH3 region from pdb 1HZH. The result showed that there are two main regions of Fc/Fc interface residues in CH3: the first region from Q347-K370 and the second region from N390-T411. Since the classical KIH mutations are in the second region, we did not consider adding further mutations here. Only the highlighted residues in the first region were considered for *in silico* mutation and analysis (via *in silico* folding stability calculations and rational design), individually and on both chains, using our criteria. Mutations were then identified that were predicted to form new or stronger interchain interactions without disrupting the binding of the Fc region to Fc receptors (FcR), the neonatal Fc receptor (FcRn) or ProA. Potential mutants were then screened *in silico* for predicted thermostability enhancement and for the modulation of pIs of the two HCs (for facile purification by ion exchange chromatography). The resulting two new mutations in the Fc domain (mutations S354Y in knob-HC and Q347E in hole-HC) were introduced to enhance the formation of heterodimer. The mutation S354Y was predicted to create an additional hydrophobic interaction between the new Y354 and the wild-type Y349 on the hole-HC, whereas the mutation Q347E was predicted to create an additional salt bridge between the negatively charged E347 and the positively charged wild-type K360 in knob-HC (Fig. 1A and B).

Based on the parental plasmids of CD20-HC, CD3-HC, the classical KIH mutations (knob (T366Y)/hole (Y407T)) were applied to form the BsAb CD20/CD3-v2, that is, CD20-hole (Y407T)/CD3-knob (T366Y). Then, two more mutations, S354Y in knob-HC (hydrophobic interaction) and Q347E in hole-HC (ionic interaction), were engineered on the CD20/CD3-v2 Fc to generate the CD20/CD3-v5b, that is, CD20-hole (Y407T, Q347E)/CD3-knob (T366Y, S354Y). These four mutations in the Fc domain (the KIH mutations and the two new mutations) are named ‘ETYY mutations’ [15]. Based on CD20/CD3-v5b, the VHs of the two HCs were exchanged to form CD20/CD3-v4b; that is, CD20-knob (T366Y, S354Y)/CD3-hole (Y407T, Q347E), in order to test which version yielded the best results (Fig. 1A). The mutant chains were verified by sequencing.

Comparison of the AEX purification of CD20/CD3-v2, CD20/CD3-v4b, CD20/CD3-5b

All three BsAbs were expressed and purified via ProA column and then AEX purification (Fig. 1C). Since the calculated isoelectric points (pIs) of the CD20 homodimer, the CD20/CD3 heterodimer, and the CD3 homodimer for v4b are 8.72, 8.44 and 7.91 respectively, and the pH of the loading and elution buffer is 9; the order of elution for the three full components should be firstly the CD20 homodimer, followed by the CD20/CD3 BsAb and finally the CD3 homodimer. The T cell activation assay from the peak

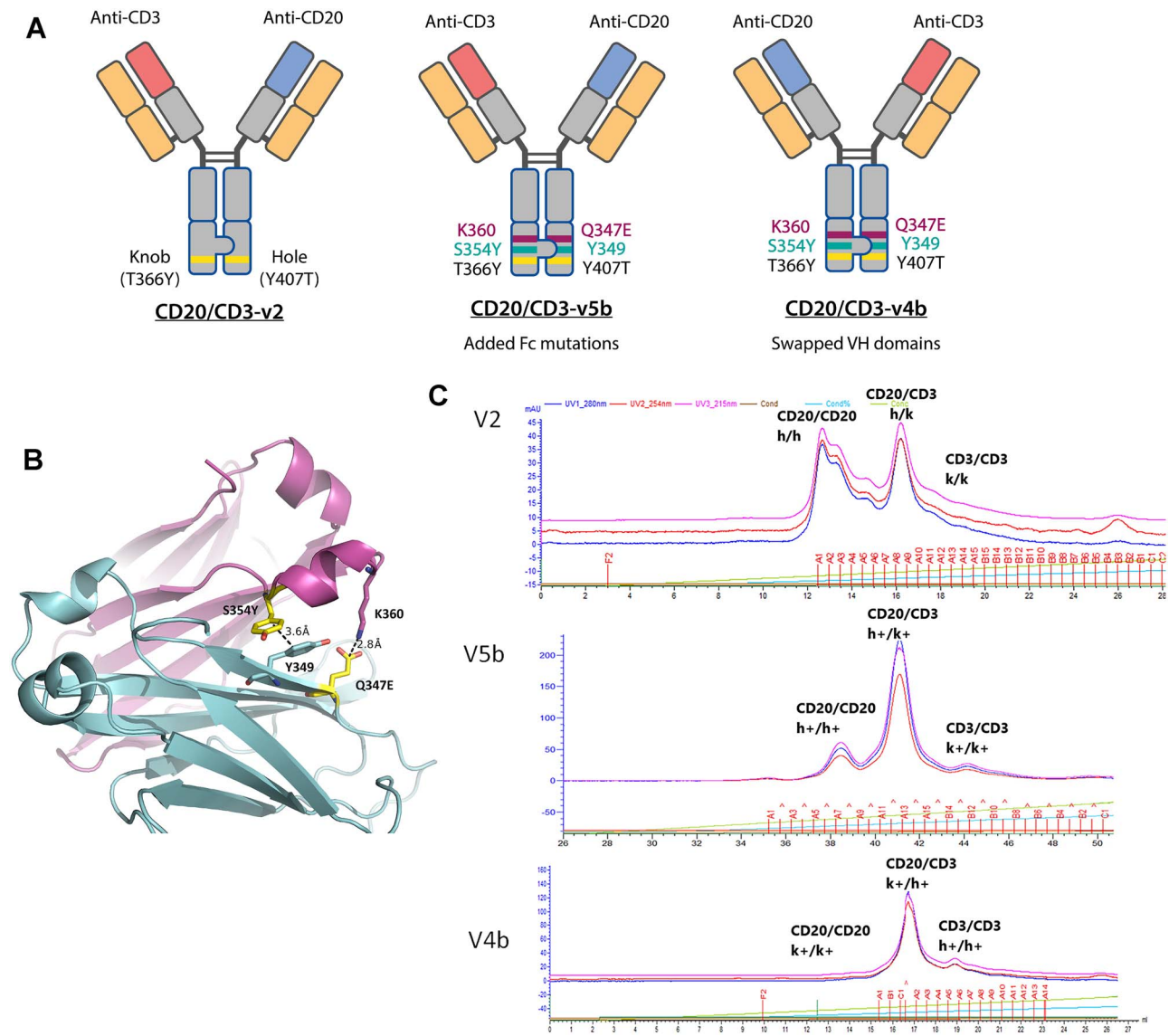


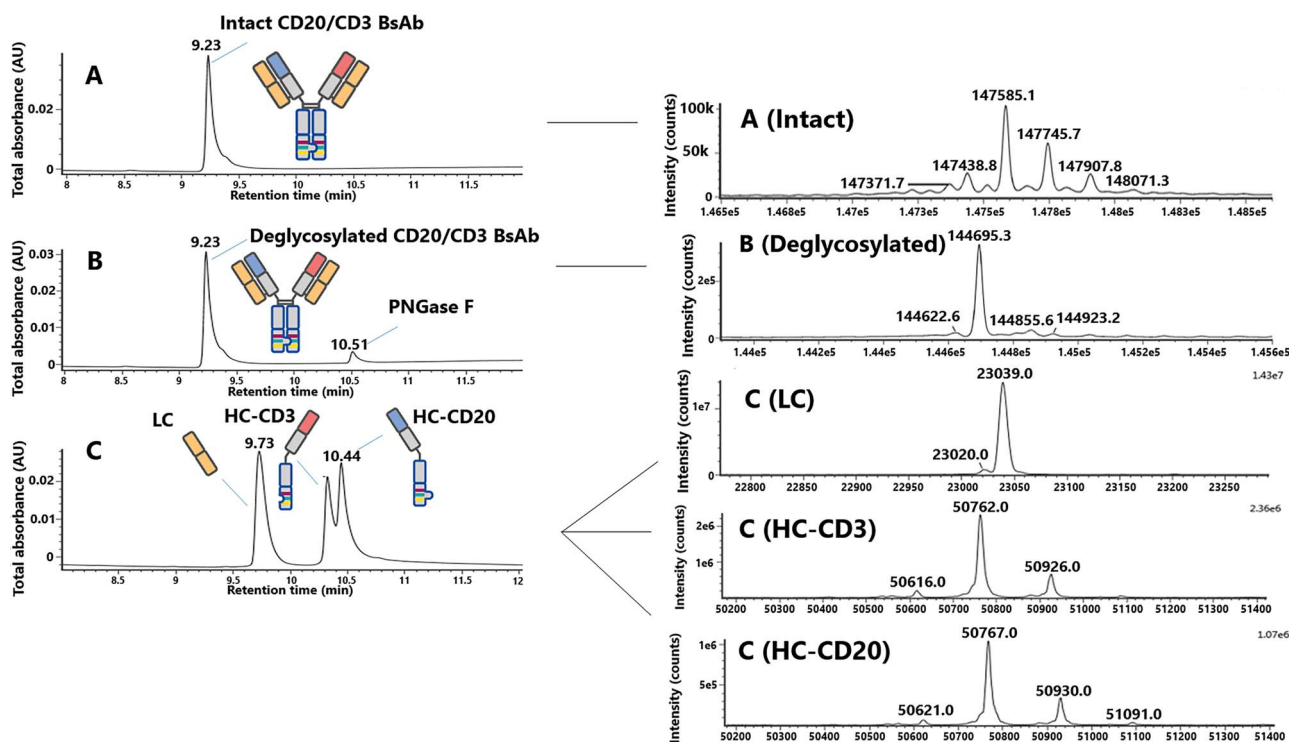
Figure 1. Demonstration of ETTY mutations and purity of the antibody Fc variants. (A) Three versions of the CD20/CD3 BsAb generated using the ETTY design. Version CD20/CD3-v2 uses the classic KIH strategy of a single pair of mutations, knob (T366Y) and hole (Y407T). For CD20/CD3-v5b, two additional mutations were added to the Fc domain according to the ETTY design, S354Y to the knob-HC and Q347E to the hole-HC, which add a predicted hydrophobic interaction and salt bridge, respectively. For CD20/CD3-v4b, the VH domains were swapped with respect to those of CD20/CD3-v5b, conferring CD3 and CD20 binding to the opposite HCs. Common LCs were used in all designs. (B) Structural model of new mutations in the ETTY design. Mutated residues are shown in yellow, wild-type residues from either CH3 domain are shown in magenta (knob CH3 domain) or cyan (hole CH3 domain). Glutamine 347 of the hole-CH3 domain (Y407T) mutated to glutamate adds a predicted salt bridge with wild-type lysine 360 of the opposite knob-CH3 domain. Serine 354 of the knob-CH3 domain (T366Y) mutated to tyrosine adds a predicted hydrophobic interaction with wild-type tyrosine 349 of the opposite hole-CH3 domain, which could involve pi-stacking. An additional hydrogen bond of 3.1 Å in length is predicted between Y349 and K360. Rotamers were predicted by Google AlphaFold v2.1.0. (C) AEX purification comparison of CD20/CD3 BsAb at v2, v4b and v5b for their product from ProA purification. In the figure, 'h' indicates the hole-CH3 (Y407T), 'k' indicates the knob-CH3 (T366Y), 'h+' indicates the new improved hole-CH3 (Y407T, Q347E), 'k+' indicates the new improved knob-CH3 (366Y, S354Y).

factions revealed that only the fractions from the second peak (for v2) and the main peak (for v4b and v5b) showed bioactivity [15], validating that these peaks in each group consisted of CD20/CD3 heterodimer. The peak before the heterodimer peak should consist of CD20 homodimer, and the peak after the heterodimer peak should consist of CD3 homodimers, according to the predicted elution order of the heterodimer and two homodimers. The CD20/CD3 heterodimer makes up <50% of the ProA purified protein

pool for v2. Compared with v2, the v5b has less CD20 homodimer and a greatly increased proportion of the CD20/CD3 heterodimer (over 80%). This indicates that the two new mutations have greatly increased the level of heterodimerization. Exchanging the two VHs of v5b generated v4b. The result shows that compared with the v5b, the v4b has a similar proportion of the CD3 homodimer but shows almost no peak for the CD20 homodimer, indicating that v4b has higher proportion of

Table 1. Deconvoluted masses of CD20/CD3 BsAb

Mass	Intact	Deglycosylated	Denatured and reduced		
			LC	HC-CD3	HC-CD20
Theoretical mass (Da)	147577.2	144688.4	23039.7	50761.9	50768.1
Detected mass (Da)	147585.1	144695.3	23039	50762	50767
Deviation (ppm)	53.5	47.7	-30.4	2	-21.7

**Figure 2.** HPLC/mass spectrometric analysis of the CD20/CD3-v4b. RP-HPLC of the CD20/CD3-v4b from AEX purification under three different treatments: (A) intact, (B) deglycosylated, (C) denature and reduced.

CD20/CD3 heterodimer. MS analysis indicated that there are 93.8% CD20/CD3 heterodimer in the ProA-purified protein pool in V4b (Table 1). In summary, out of the three versions, v4b has the highest proportion of CD20/CD3 heterodimers.

CD20/CD3-v4b structure confirmation by RP-MS

Through RP-MS based mass analysis, the structure of CD20/CD3-v4b linked by two identical LCs and two distinct HCs was confirmed (Fig. 2 and Table 1). All the detected masses were consistent with the theoretical ones. This also indicated that via the second ion exchange purification, very high purity of the heterodimer can be achieved.

ETYY mutations do not affect FcRn binding in CD20/CD3-v4b

The FcRn can bind to an antibody in weakly acidic conditions (pH 6.0) and extend its half-life by inhibiting

protease-mediated hydrolysis. Therefore, FcRn binding affinity analysis was performed to assess the potential impact of the ETYY mutations on the antibody half-life. The K_D value of this interaction was calculated by the Biacore T200 Evaluation Software and measured to be 512 nM, which is close to the normal value (540 ~ 737 nM) of the Fc KD [21], demonstrating that the ETYY mutations on Fc of CD20/CD3-v4b do not impair the FcRn binding activity. The binding curves are shown in Figure 3.

ETYY mutations retain high thermostability and low aggregation propensity in CD20/CD3-v4b

DSF/SLS and DLS assays were applied to check the thermostability and aggregation propensity of the CD20/CD3-v4b using the UNcle system (Unchained labs). The results showed that the T_{m1} and T_{m2} were 66.3 and 79.8°C, respectively, whereas the T_{agg266} and T_{agg473} were 70.5 and 70.7°C, respectively (Fig. 4A). In addition, DSC was performed for the AEX-purified antibody, and the results

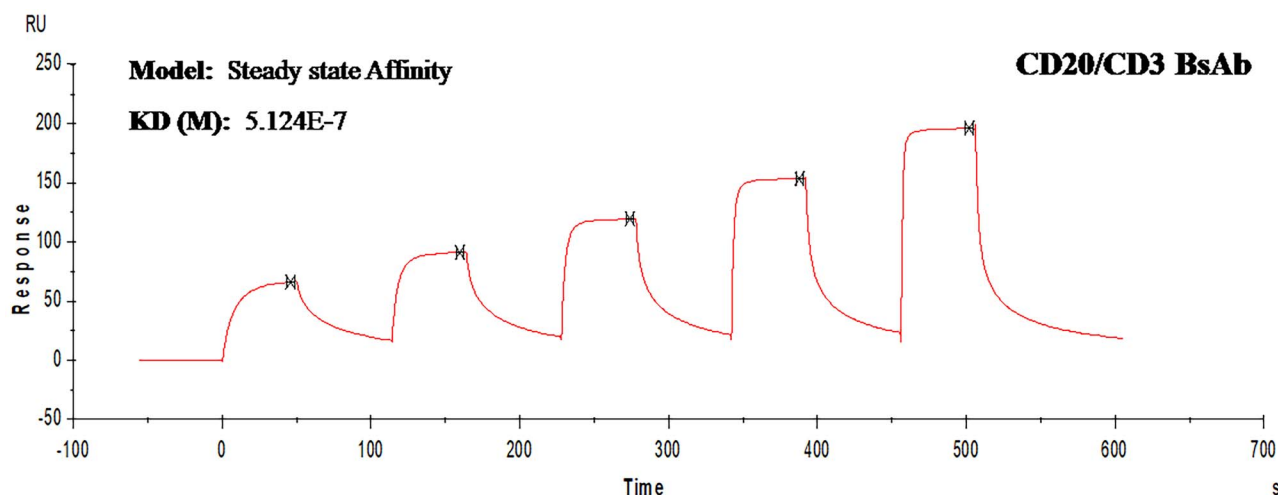


Figure 3. Sensorgram of CD20/CD3-v4b BsAb binding to human FcRn by single cycle kinetics assay. Conc1: 62.5 nM, Conc2: 125 nM, Conc3: 250 nM, Conc4: 500 nM, Conc5: 1000 nM.

show that they have two transition temperatures at 65.41 and 73.59°C, respectively (Fig. 4B), consistent with the result obtained from DSF. Therefore, all our data show that the CD20/CD3-v4b has high thermostability. The DLS assay (at 25°C) also revealed that only one peak was observed (100% of the whole mass) with a mode diameter of 9.68 nm, consistent with the average size of an IgG molecule. The polydispersity index (PDI) is 0.121, lower than the upper limit value of 0.2 for the range, suggesting low aggregation propensity for the CD20/CD3-v4b antibody (Fig. 4C).

ETYY mutations retain favorable physicochemical properties of other BsAb/TsAb

The ETYY mutations were also applied to a BsAb PDL1/CD55 and trispecific antibody (TsAb) cMet/EGFR, and both show high heterodimer percentages and favorable physicochemical properties, as measured at the chemistry, manufacturing, and controls (CMC) management level. Their main characterizations are listed in Table 2. The data show that with ETYY mutations, both PDL1/CD55 and cMet/EGFR have high thermostability (DSC data in Table 2) and low aggregation propensity (size exclusion high-performance liquid chromatography (SE-HPLC) and DLS data in Table 2), while at the same time retaining the FcRn binding activity (Table 2). The CD20/CD3 and cMet/EGFR antibodies have yielded favorable animal study results and are under clinical trial now [22]. Please note that in order to enhance the antibody-dependent cellular cytotoxicity (ADCC) of the cMet/EGFR TsAb, mutation S239D/I332E in the CH2 domain was also applied to the antibody [23]. This mutation was reported to reduce the T_m of the antibody by >20°C [24], which is most probably the reason why a lower T_m for cMet/EGFR was measured (Table 2). This shows that ETYY is a broadly applicable Fc modification that could enhance the physicochemical properties of the antibodies.

DISCUSSION

The classic KIH (knob(T366Y)/hole (Y407T)) is a successful strategy for increasing the heterodimerization of BsAbs. Here we show the introduction of two new mutations S354Y in knob-HC and Q347E in hole-HC that are predicted to produce new hydrophobic and ionic interactions, respectively. These mutations, named ETYY, were identified by computational design and further enhance the interactions of the two HCs of the CD20/CD3 BsAb. The results indicate that adding the two new ETYY mutations greatly increases the percentage of CD20/CD3 hybrid, reduces the percentage of the homodimers. Heterodimer with high purity can then be obtained via AEX purification. Functional validation by the T cell activation assays shows that CD20/CD3-v4b (with the ETYY mutations) successfully retains the activity of the BsAb both at Fab and Fc regions. Upon further characterization, we show that the CD20/CD3-v4b hybrid has high thermostability and low aggregation potential. In summary, adding two new mutations to the classic KIH on the Fc of a BsAb (S354Y in knob-HC and Q347E in hole-HC) and generating the ETYY mutation combination enhances heterodimerization while retaining the original function and preserving favorable physicochemical properties. This novel design could be utilized in the production of next-generation BsAbs with higher yields and simpler purification.

There are at least three factors that determine the final proportion of heterodimer in the ProA purified pools. First, Fc engineering designed to enhance heterodimer formation (such as KIH and ETYY strategies) affect the proportion of heterodimer via mutations that increase affinity of the two different HCs for each other, decrease affinity of each HC to itself (disfavoring homodimer formation) or both. Secondly, heterodimer formation depends on the rate of translation of each HC and the stability and aggregation propensity of each HC in the endoplasmic reticulum after translation. If the rates of translation and stabilities of the two HCs are unequal, heterodimer formation may be

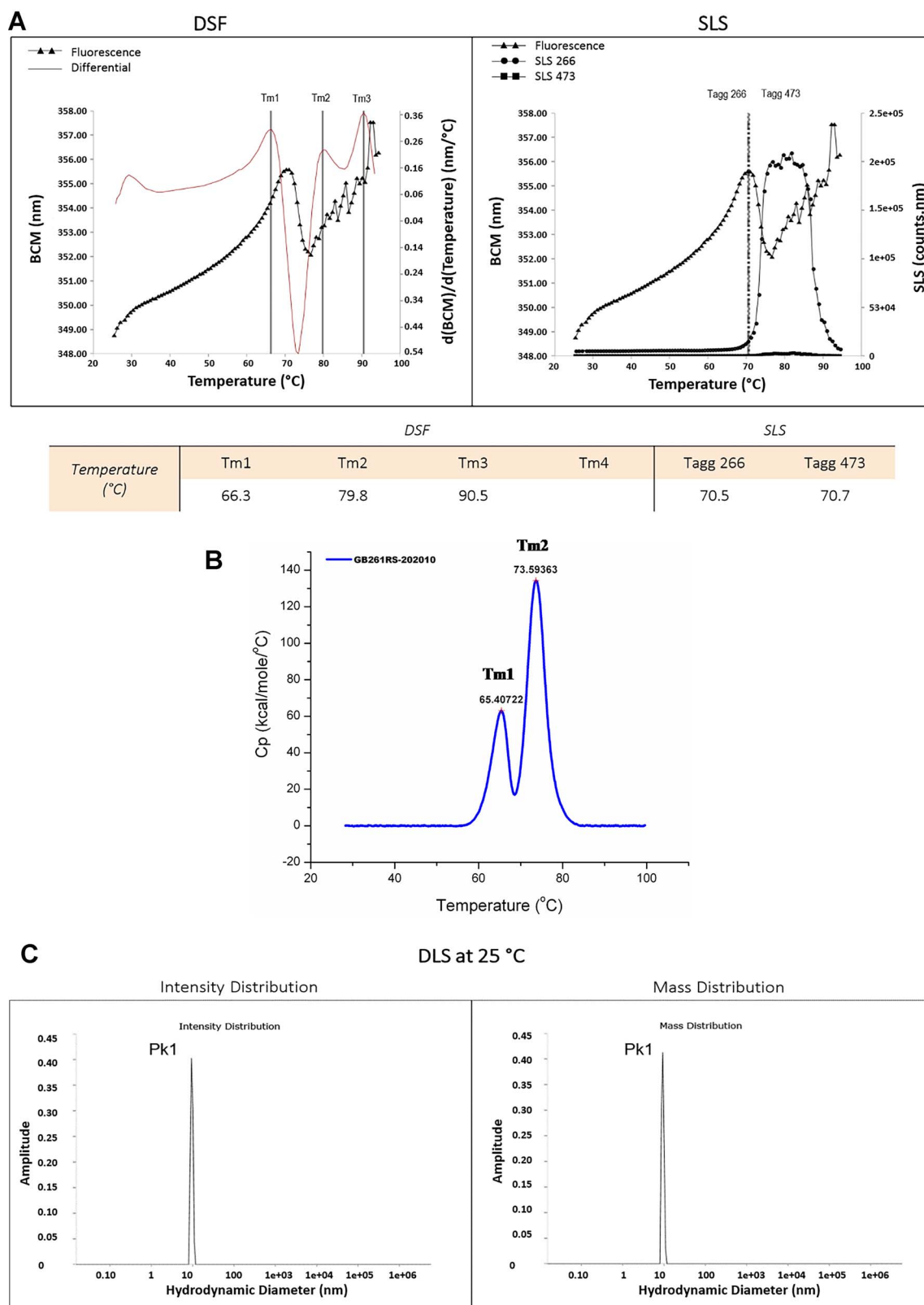


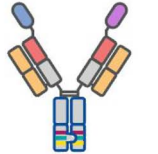


Figure 4. Thermostability and aggregation propensity of CD20/CD3-IgG-v4b. (A) Results from the DSF and SLS assays. (B) Results from the DSC assay. (C) Results from the DLS assay.

Table 2. Characterization of three multi-specific antibodies with ETTY mutations

BsAb/TsAb		CD20/CD3 (BsAb)	PDL1/CD55 (BsAb)	cMet/EGFR (TsAb)
Topology				
Heterodimer percentage (%)		93.8	69	95.0
SE-HPLC	Monomer (%)	99.2	99.2	98.8
	HMW (%)	0.5	0.3	0.4
	LMW (%)	0.3	0.5	0.8
Thermal stability (DSC)	Tm1 (°C)	65.41	67.27	50.15*
	Tm2 (°C)	73.59	72.78	58.97*
DLS	Number Mean (d.nm)	10.32	10.41	12.413
	PDI	0.036	0.056	0.097
FcRn binding activity	KD (M)	5.12E-07	5.98E-07	5.58E-07

*Decreased probably due to added 'S239D/I332E' mutation in CH2. Two ovals in different color noted in cMet/EGFR topology correspond to two different VHH (camelid nanobody) domains targeting different epitopes of cMet.

reduced. In order to circumvent this problem, the third factor, the ratio of plasmids containing a copy of each HC gene used during transfection, may be adjusted for optimal heterodimer formation.

We designed another BsAb and a TsAb using this ETTY design, and their properties are summarized in Table 2. In the case of PDL1/CD55 BsAb, the difference in pI between the two HCs was very small, and reduced electrostatic steering effects may contribute to the lower heterodimer percentage. Additionally, the plasmid ratio used for transfection was near 1:1 (HC1:HC2) and had not yet been optimized; thus, heterodimer yields would likely be much higher after optimization. Even without plasmid ratio optimization, however, this antibody produced a heterodimer proportion high enough to be suitable for industrial manufacturing and likely increased the heterodimer percentage over the classic KIH mutations alone. In the case of cMet/EGFR TsAb, a heterodimer percentage of 95.0% was obtained after plasmid ratio optimization. This suggests that the ETTY design has generality and may be applied to other BsAbs and TsAbs, yielding favorable results.

Other strategies to improve heterodimer formation and recovery that have been recently described include strand-exchange engineered domain (SEED) [25, 28], the XmAb bispecific platform [26, 29], the addition of disulfide linkages at the CH3–CH3 domain interface [27, 29], additional steric 'knob-and-hole' mutations identified by phage display [19, 29] and engineering for the separation of isoelectric points between the two HCs in order to facilitate purification by ion exchange [26, 29]. The SEED method utilizes

a steric-based strategy that replaces patches at the CH3–CH3 domain interface with homologous regions from IgA for novel complementarity, improving heterodimerization to 85–95% of the purified protein pool. This method has been shown to reduce thermostability in some designs [30]. In the XmAb platform, mutations add a salt bridge and a hydrogen bond; however, a wild-type salt bridge and hydrogen bond were simultaneously removed, resulting in a near net-zero change in CH3–CH3 interactions in the heterodimer. It is purported to add one electrostatic repulsion interaction in each homodimer however, which is thought to disfavor homodimer formation. The XmAb platform also modulates the isoelectric points between the two HCs. Yields of the BsAb heterodimer for this method have been reported up to 95.1%, with a slight reduction in T_m for the CH3 regions by about 6°C, as reported [25]. In a patent invented by Ting Xu [31] and described in the paper 'Structural basis of a novel heterodimeric Fc for bispecific antibody production' [32], a comprehensive engineering on CH3 domain was investigated. Among all the 18 claimed CH3 engineering combinations, one combination (with two mutations in Chain A and 4 mutations in Chain B) led to the heterodimer percentage over 90% at the optimized co-transfection ratio in the case. The antibody produced using this design was reported to retain high thermostability. This strategy shows promise, and while only one example antibody was produced using this combination of mutations, it would be desirable to produce more examples in order to test the generality of the design.

Unlike other reported methods, our ETTY mutations and overall design described here combines an added

salt bridge, an added hydrophobic interaction which may involve pi-stacking, steric mutations (from the classic KIH mutations and from the S354Y mutation), a common LC to circumvent LC mispairing and the modulation of isoelectric points between the two HCs. Further, rotamers predicted by Google AlphaFold v2.1.0 suggest there may be an additional interchain hydrogen bond between wild-type residues Y349 and K360 in the heterodimer that is not present in the wild-type antibody or predicted in either homodimer. The proximity of these three additional interchain interactions to each other and the predicted new sidechain packing suggests there may be added structural rigidity in this region in addition to tighter binding between the two HCs; we hypothesize that this may enhance heterodimer formation and thermostability of BsAbs produced using our ETTY design. Yields of up to 94% heterodimer have been obtained experimentally.

This is a case study in the use of computational design for antibody engineering within the Fc region, which shows success in the development of a new and robust BsAb platform based on mutations identified *in silico*. This ETTY platform is suitable for the design of therapeutic antibodies with improved manufacturability. With the advent of new and highly accurate protein structure prediction software applying deep learning such as Google AlphaFold [33] and RoseTTAFold [34, 35], advancements in software using energy functions [36] and new hybrid approaches [37], and with improving accuracy in the prediction of stabilizing mutations [38, 39], antibody engineering is on the verge of an exciting and critical step in the evolution of the field. With this regard, computer-based and computer-aided approaches will become increasingly important in this burgeoning field [40–45].

AUTHOR CONTRIBUTIONS

B.W. and J.L. designed and performed experiments, analyzed data and drafted the manuscript. M.R.H. and S.G.K. drafted the manuscript. M.W. performed experiments and drafted the manuscript. M.M. performed experiments. W.C. performed experiments and analyzed data. Y.L. conceived the idea, performed computer-aided antibody design, drafted the manuscript and provided leadership to operations and projects related to the contents.

ACKNOWLEDGEMENT

The authors appreciate and would like to thank all contributors from Ab Studio, Inc. for their valuable support in this project.

FUNDING

Funding for this study was received from Ab Studio, Inc. and Genor Biopharma Co. Ltd., a JHBP company.

CONFLICT OF INTEREST

B.W., M.R.H., M.W., W.C. and S.G.K. are employees of Ab Studio, Inc. J.L. and M.M. are employees of Genor Biopharma Co. Ltd. Y.L. is the Founder and President of

Ab Studio Inc., and Founder and Chief Executive Officer of Ab Therapeutics, Inc. Ab Studio, Inc., Ab Therapeutics, Inc. and Genor Biopharma Co. Ltd. commercially develop therapeutic antibodies for human diseases.

DATA AVAILABILITY

Please contact Dr Yue Liu (yue.liu@antibodystudio.com) for original data.

ETHICS AND CONSENT

Not applicable.

ANIMAL RESEARCH

Not applicable.

REFERENCES

- Nisonoff, A, Rivers, MM. Recombination of a mixture of univalent antibody fragments of different specificity. *Arch Biochem Biophys* 1961; **93**: 460–2.
- Crick, FHC. Is α -keratin a coiled coil? *Nature* 1952; **170**: 882–3.
- Ridgway, JB, Presta, LG, Carter, P. “Knobs-into-holes” engineering of antibody CH3 domains for heavy chain heterodimerization. *Protein Eng* 1996; **9**: 617–21.
- Zhang, X, Yang, Y, Fan, D *et al*. The development of bispecific antibodies and their applications in tumor immune escape. *Exp Hematol Oncol* 2017; **6**: 12.
- Schaefer, W, Regula, JT, Bahner, M *et al*. Immunoglobulin domain crossover as a generic approach for the production of bispecific IgG antibodies. *Proc Natl Acad Sci* 2011; **108**: 11187–92.
- Marvin, JS, Zhu, Z. Recombinant approaches to IgG-like bispecific antibodies. *Acta Pharmacol Sin* 2005; **26**: 649–58.
- Kontermann, RE. Recombinant bispecific antibodies for cancer therapy. *Acta Pharmacol Sin* 2005; **26**: 1–9.
- Merchant, M, Ma, X, Maun, HR *et al*. Monovalent antibody design and mechanism of action of onartuzumab, a MET antagonist with tumor activity as a therapeutic agent. *Proc Natl Acad Sci* 2013; **110**: E2987–96.
- Klein, C, Schaefer, W, Regula, JT *et al*. Engineering therapeutic bispecific antibodies using CrossMab technology. *Methods* 2019; **154**: 21–31.
- Mazor, Y, Oganessian, V, Yang, C *et al*. Improving target cell specificity using a novel monovalent bispecific IgG design. *MAbs* 2015; **7**: 377–89.
- Klein, C, Schaefer, W, Regula, JT. The use of CrossMab technology for the generation of bi- and multispecific antibodies. *MAbs* 2016; **8**: 1010–20.
- Gunasekaran, K, Pentony, M, Shen, M *et al*. Enhancing antibody Fc heterodimer formation through electrostatic steering effects. *J Biol Chem* 2010; **285**: 19637–46.
- Spiess, C, Merchant, M, Huang, A *et al*. Bispecific antibodies with natural architecture produced by co-culture of bacteria expressing two distinct half-antibodies. *Nat Biotechnol* 2013; **31**: 753–8.
- Xu, Y, Lee, J, Tran, C *et al*. Production of bispecific antibodies in “knobs-into-holes” using a cell-free expression system. *MAbs* 2015; **7**: 231–42.
- Cai, W, Dong, J, Gallolu Kankanamalage, S *et al*. Biological activity validation of a computationally designed rituximab/CD3 T cell engager targeting CD20+ cancers with multiple mechanisms of action. *Antibody Therapeutics* 2021; **4**: 228–41.
- Jackman, J, Chen, Y, Huang, A *et al*. Development of a two-part strategy to identify a therapeutic human bispecific antibody that inhibits IGE receptor signaling. *J Biol Chem* 2010; **285**: 20850–9.
- Alt, M, Müller, R, Kontermann, RE. Novel tetravalent and bispecific IgG-like antibody molecules combining single-chain

- diabodies with the immunoglobulin γ 1 Fc or CH3 region. *FEBS Lett* 1999; **454**: 90–4.
18. Germain, C, Campigna, E, Salhi, I *et al*. Redirecting NK cells mediated tumor cell lysis by a new recombinant bifunctional protein. *Protein Eng Design Selection* 2008; **21**: 665–72.
 19. Atwell, S, Ridgway, JB, Wells, JA *et al*. Stable heterodimers from remodeling the domain interface of a homodimer using a phage display library. *J Mol Biol* 1997; **270**: 26–35.
 20. Zhu, Z, Presta, LG, Zapata, G *et al*. Remodeling domain interfaces to enhance heterodimer formation. *Protein Sci* 1997; **6**: 781–8.
 21. Abdiche, YN, Yeung, YA, Chaparro-Riggers, J *et al*. The neonatal Fc receptor (FcRn) binds independently to both sites of the IgG homodimer with identical affinity. *MAbs* 2015; **7**: 331–43.
 22. Xiao, Y, Ganju, V (2021-2025). *A Safety, Tolerability, Pharmacokinetics and Efficacy Study of GB261 in B-Cell NHL and CLL*. Identifier NCT04923048. <https://clinicaltrials.gov/ct2/show/study/NCT04923048>
 23. Lazar, GA, Dang, W, Karki, S *et al*. Engineered antibody Fc variants with enhanced effector function. *Proc Natl Acad Sci* 2006; **103**: 4005–10.
 24. Liu, Z, Gunasekaran, K, Wang, W *et al*. Asymmetrical Fc engineering greatly enhances antibody-dependent cellular cytotoxicity (ADCC) effector function and stability of the modified antibodies. *J Biol Chem* 2014; **289**: 3571–90.
 25. Davis, JH, Aperlo, C, Li, Y *et al*. SEEDbodies: fusion proteins based on strand-exchange engineered domain (SEED) CH3 heterodimers in an Fc analogue platform for asymmetric binders or immunofusions and bispecific antibodies. *Protein Eng Des Sel* 2010; **23**: 195–202.
 26. Moore, GL, Bennett, MJ, Rashid, R *et al*. A robust heterodimeric Fc platform engineered for efficient development of bispecific antibodies of multiple formats. *Methods* 2019; **154**: 38–50.
 27. Merchant, AM, Zhu, Z, Yuan, JQ *et al*. An efficient route to human bispecific IgG. *Nat Biotechnol* 1998; **16**: 677–81.
 28. Liu, H, Saxena, A, Sidhu, SS *et al*. Fc engineering for developing therapeutic bispecific antibodies and novel scaffolds. *Front Immunol* 2017; **8**.
 29. Wang, Q, Chen, Y, Park, J *et al*. Design and production of bispecific antibodies. *Antibodies* 2019; **8**: 43.
 30. Muda, M, Gross, AW, Dawson, JP *et al*. Therapeutic assessment of SEED: a new engineered antibody platform designed to generate mono- and bispecific antibodies. *Protein Eng Design Selection* 2011; **24**: 447–54.
 31. Xu, T, Jiangsu Alphamab Biopharmaceuticals Co Ltd, SUZHOU ALPHAMAB Co Ltd. Heterodimer molecule based on CH3 domain, and preparation method and use thereof. United States patent US 11,168,149, 2021 Nov 9.
 32. Wei, H, Cai, H, Jin, Y *et al*. Structural basis of a novel heterodimeric Fc for bispecific antibody production. *Oncotarget* 2017; **8**: 51037–49.
 33. Jumper, J, Evans, R, Pritzel, A *et al*. Highly accurate protein structure prediction with AlphaFold. *Nature* 2021; **596**: 583–9.
 34. Baek, M, DiMaio, F, Anishchenko, I *et al*. Accurate prediction of protein structures and interactions using a three-track neural network. *Science* 2021; **373**: 871–6.
 35. Wang, J, Lisanza, S, Juergens, D *et al*. Scaffolding protein functional sites using deep learning *Science* 2022; **377**: 387–394.
 36. Kuhlman, B, Bradley, P. Advances in protein structure prediction and design. *Nat Rev Mol Cell Biol* 2019; **20**: 681–97.
 37. Norn, C, Wicky, BIM, Juergens, D *et al*. Protein sequence design by conformational landscape optimization. *Proc Natl Acad Sci* 2021; **118**: e2017228118.
 38. Nisthal, A, Wang, CY, Ary, ML *et al*. Protein stability engineering insights revealed by domain-wide comprehensive mutagenesis. *Proc Natl Acad Sci* 2019; **116**: 16367–77.
 39. Barlow, KA, Conchúir, SÓ, Thompson, S *et al*. Flex ddG: Rosetta ensemble-based estimation of changes in protein–protein binding affinity upon mutation. *J Phys Chem B* 2018; **122**: 5389–99.
 40. Lewis, SM, Wu, X, Pustilnik, A *et al*. Generation of bispecific IgG antibodies by structure-based design of an orthogonal Fab interface. *Nat Biotechnol* 2014; **32**: 191–8.
 41. Lee, J, Der, BS, Karamitros, CS *et al*. Computer-based engineering of thermostabilized antibody fragments. *AIChE J* 2019; **66**: e16864.
 42. Froning, K, Maguire, J, Sereno, A *et al*. Computational stabilization of T cell receptors allows pairing with antibodies to form bispecifics. *Nat Commun* 2020; **11**: 2330.
 43. Wang, B, Gallolu Kankanamalage, S, Dong, J *et al*. Optimization of therapeutic antibodies. *Antibody Ther* 2021; **4**: 45–54.
 44. Dong, J, Huang, B, Jia, Z *et al*. Development of multi-specific humanized llama antibodies blocking SARS-CoV-2/ACE2 interaction with high affinity and avidity. *Emerg Microbes Infect* 2020; **9**: 1034–6.
 45. Dong, J, Huang, B, Wang, B *et al*. Development of humanized tri-specific nanobodies with potent neutralization for SARS-CoV-2. *Sci Rep* 2020; **10**: 17806.